



OPEN ACCESS

EDITED BY
Phoebe Koundouri,
Athens University of Economics and
Business, Greece

REVIEWED BY
Shanzhong Qi,
Shandong Normal University, China
Yixiong He,
Zhejiang Ocean University, China

*CORRESPONDENCE
Chunjuan Wang
✉ cjw@fio.org.cn

RECEIVED 19 November 2025
REVISED 17 March 2026
ACCEPTED 18 March 2026
PUBLISHED 02 April 2026

CITATION

Xu C, Wang C, Liu D, Zhang Z, Li Y and
Li Z (2026) Evolution of carbon sink
patterns and spatial planning suitability in
the Qingdao Coastal Zone based on the
coupled InVEST–PLUS model.
Front. Mar. Sci. 13:1749473.
doi: 10.3389/fmars.2026.1749473

COPYRIGHT

© 2026 Xu, Wang, Liu, Zhang, Li and Li.
This is an open-access article distributed
under the terms of the [Creative
Commons Attribution License \(CC BY\)](https://creativecommons.org/licenses/by/4.0/).
The use, distribution or reproduction in
other forums is permitted, provided the
original author(s) and the copyright
owner(s) are credited and that the
original publication in this journal is
cited, in accordance with accepted
academic practice. No use, distribution
or reproduction is permitted which does
not comply with these terms.

Evolution of carbon sink patterns and spatial planning suitability in the Qingdao Coastal Zone based on the coupled InVEST–PLUS model

Chunxia Xu¹, Chunjuan Wang^{2*}, Dahai Liu³, Zhiwei Zhang²,
Yanping Li² and Zheng Li²

¹College of Ocean Science and Engineering, Shandong University of Science and Technology, Qingdao, China, ²Key Laboratory of Coastal Zone Science and Integrated Management, First Institute of Oceanography, Ministry of Natural Resources, Qingdao, China, ³School of Public Administration, Renmin University of China, Beijing, China

To support the “dual-carbon” strategy and develop a carbon-sink-oriented coastal spatial planning framework, this study applies the coupled InVEST–PLUS model to Qingdao using 30 m resolution land-use data. Six spatial drivers (DEM, slope, GDP, population, road, and water proximity) are used to simulate land-use change and evaluate its impact on carbon storage. Model validation results indicate that the PLUS model shows good performance ($Kappa \approx 0.79$, $FoM = 0.168$). The results indicate that (1) during 2010–2020, land-use patterns in the study area changed markedly, characterized by a decrease in farmland and an expansion of architecture area, while forest increased slightly and overall ecological land declined. (2) Total carbon storage dropped from 5.3174×10^7 t (2010) to 5.2749×10^7 t (2020), with a net loss of 4.25×10^5 t. Spatially, carbon storage showed a “clustered-high, contiguous-medium, radial-low” pattern. (3) DEM and water proximity primarily drove the expansion of farmland, forest, grassland, and waters, while population density and DEM dominated architecture growth; bare land expansion was mainly driven by population. Based on these findings, carbon storage transfer pathways are quantified, providing a scientific basis for low-carbon-oriented territorial spatial governance in coastal zones.

KEYWORDS

carbon storage, InVEST model, PLUS model, spatial planning, spatiotemporal evolution

1 Introduction

Global climate warming has led to increasingly frequent extreme climate events and rising concentrations of greenhouse gases, which have become major challenges constraining socio-economic development and ecosystem stability (Cramer et al., 2018). The Sixth Assessment Report of the IPCC (Intergovernmental Panel on Climate Change) states that human activities have driven atmospheric CO₂ concentrations to their highest levels in two million years. Against this backdrop, the deep integration of carbon sink enhancement into territorial spatial planning has become a critical pathway for achieving

the “dual-carbon” goals and coordinating ecological protection with regional development. As a typical land–sea interaction system, the coastal zone exhibits both carbon sink and carbon source characteristics. The evolution of carbon storage directly determines the ecological suitability of spatial planning and serves as a key link between ecological conservation and regional development, while also playing an important role in regional climate regulation (Dybala et al., 2019). The dynamics of carbon storage in terrestrial ecosystems are a core component of climate regulation. In coastal zones, high-intensity land-use transitions, including urban expansion and the conversion of ecological land, have become dominant drivers of carbon storage change. Systematically revealing the spatiotemporal evolution of carbon storage is therefore not only a scientific requirement for advancing carbon-cycle theory in land–sea interaction regions, but also a key technical foundation for establishing a carbon-sink-oriented coastal spatial planning framework (Mallapaty, 2020).

Qingdao’s coastal zone is located in the southern part of the Shandong Peninsula and integrates multiple functions, including port-based economic development, coastal tourism, and ecological conservation, making it a typical region characterized by strong interactions between human activities and natural processes (Liu et al., 2017). This study focuses on Qingdao as an integrated coastal urban system. Operationally, the “coastal region” is defined as the entire municipal administrative area, reflecting the pervasive influence of port-oriented development and land–sea interactions on the city’s land-use and carbon patterns. This definition ensures consistency with the available data and planning frameworks. The terms “Qingdao” and “Qingdao coastal region” are used synonymously in this study. In the context of rapid urbanization and industrial restructuring, the region faces dual pressures from intensified economic development and carbon sink conservation. There remains a notable mismatch between existing research and the needs of coastal spatial planning. On the one hand, the long-term spatiotemporal evolution of carbon storage at the scale of the entire coastal zone has not yet been systematically characterized. Most existing studies focus on single wetland types or local-scale areas, which limits their capacity to support integrated planning decisions (Hou et al., 2012). On the other hand, intensive land-use transformations driven by land–sea interactions have resulted in highly unstable carbon pool structures. The coupled driving mechanisms of natural and socio-economic factors remain insufficiently understood, making it difficult to distinguish their relative contributions and nonlinear interactions (Duan et al., 2025). As a result, existing studies do not provide sufficient quantitative support for defining differentiated planning thresholds or optimizing land-use configurations. Moreover, most studies primarily focus on current carbon storage assessments and lack dynamic scenario simulations based on land-use change trends. For example, the Jiaozhou Bay salt marsh carbon sink monitoring pilot only quantifies current carbon sink capacity, which limits its ability to inform medium- and long-term ecological planning and hinders the achievement of a precise balance between carbon sink protection and spatial development.

Land-use and land-cover change in coastal regions is a core driver of carbon storage variation (Zhu et al., 2021; Nie et al., 2020;

Lai et al., 2016). Existing land-use and land-cover products can accurately depict land-use patterns across different time periods and provide reliable baseline data for regional carbon storage estimation. In coastal regions characterized by rapid urban expansion and strong land–sea interactions, the limitations of such products become particularly evident. As observation-based outcome data, existing LULC products mainly reflect the final states of land-use change and cannot capture the dynamic conversion processes among different land-use types. Moreover, static classification results cannot distinguish real changes from apparent differences caused by classification uncertainty, and they do not reveal the contribution mechanisms of different natural and socio-economic driving factors to land-use change. Therefore, relying solely on multi-temporal LULC products is insufficient to support scenario-based simulations of carbon storage change and planning-oriented analyses. It is therefore necessary to introduce land-use simulation models that explicitly represent land-use transition processes and their driving mechanisms. At the regional scale, carbon storage assessments are inevitably affected by both land-use classification errors and uncertainties in carbon density parameters. The approach adopted in this study is intended to characterize temporal trends in carbon storage under existing data constraints and to provide relative change patterns and scenario-based comparisons, rather than to achieve absolute pixel-level accuracy.

Currently, in addition to field-based measurements and statistical inventories, model-based simulation is widely used for regional carbon storage estimation. The carbon storage module of the InVEST (Integrated Valuation of Ecosystem Services and Tradeoffs) model is characterized by flexible parameterization, robust performance, and an effective representation of ecosystem service functions (Liu et al., 2025), and has therefore been widely applied in regional carbon storage assessments. A single model is insufficient for conducting dynamic scenario simulations and projections. The PLUS (Patch-generating Land Use Simulation) model can capture both the spatial pattern characteristics of land-use change and the responses to multiple driving factors, and it has demonstrated strong performance in simulating urban expansion and ecological land-use transitions (Wan et al., 2025). In recent years, the coupled InVEST–PLUS model has been widely applied and validated in the Dongting Lake Basin (Hou et al., 2025), the Huaihe River Basin (Yang et al., 2024), the Yihe River Basin (Zhang et al., 2025), and the Yellow River Delta (Tang et al., 2024), demonstrating strong reliability and predictive capability in quantifying the spatial distribution of land use and carbon storage.

In addition to ensuring the continuity and comparability of multi-source datasets, the study period from 2010 to 2020 was selected to align with key milestones in national and local planning cycles. Specifically, 2010 serves as the baseline year prior to the implementation of the 12th Five-Year Plan (2011–2015), representing the pre-planning conditions of land use and carbon storage. The year 2015 corresponds to the completion of the 12th Five-Year Plan and allows for an evaluation of the combined effects of urban expansion and ecological governance during this stage. The year 2020 marks the completion of the 13th Five-Year Plan (2016–2020) and is used as the validation benchmark for the

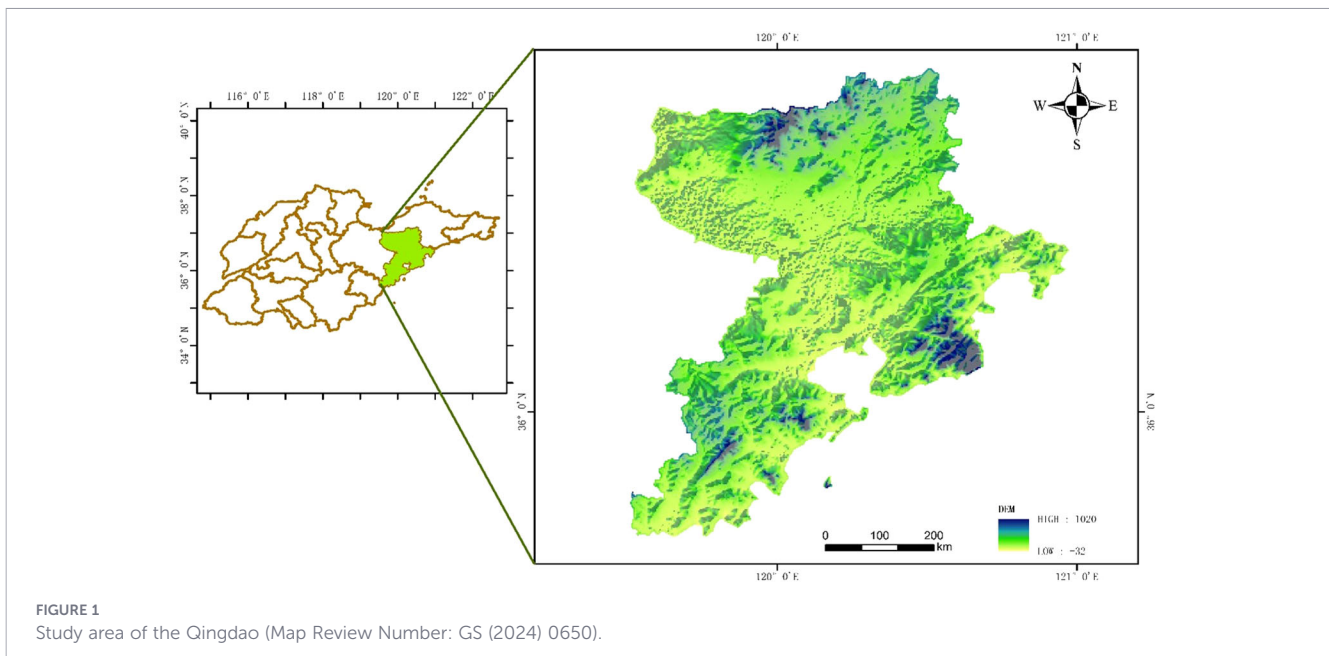


FIGURE 1 Study area of the Qingdao (Map Review Number: GS (2024) 0650).

coupled InVEST-PLUS simulation. Therefore, the period from 2010 to 2020 provides a complete observation window covering the pre-, mid-, and post-planning phases under consistent data conditions, thereby supporting policy-relevant interpretations of Qingdao’s urbanization process and its stage-wise carbon storage dynamics, as well as robust model validation.

Based on this framework, this study employs the coupled InVEST-PLUS model to systematically reveal the spatiotemporal evolution of carbon storage in Qingdao’s coastal zone from 2010 to 2020, to identify the key driving factors influencing carbon storage change, and to evaluate the applicability of the PLUS model for carbon storage scenario simulations in coastal regions. The contributions of multiple driving factors, including the Digital Elevation Model (DEM), slope, gross domestic product (GDP), population, road proximity, and water proximity, are quantitatively analyzed. The proposed approach provides diagnostic and simulation tools for optimizing territorial spatial patterns and carbon management in Qingdao’s coastal zone, and offers scientific support for land-use optimization, ecological restoration planning, and carbon sink enhancement strategies. Furthermore, it serves as a technical reference for establishing carbon-sink-oriented spatial planning frameworks in other coastal regions. The study is guided by the following three objectives:

- (1) To systematically quantify the spatiotemporal evolution of carbon storage induced by land-use transitions in Qingdao’s coastal zone from 2010 to 2020, to identify the key land-use types responsible for carbon loss and gain and their spatial distributions, and to provide targeted support for zoned territorial spatial planning and regulation.
- (2) To evaluate the simulation accuracy and applicability of the PLUS model, based on existing land-use products, for carbon storage scenario projections, and to verify whether it can support medium- to long-term carbon storage forecasting at the planning scale.
- (3) This objective aims to quantitatively analyze the relative contributions of different natural and socio-economic driving

factors, including terrain, population, economic activity, and transportation conditions, to land-use transitions and carbon storage changes, and to elucidate the mechanisms of carbon storage variation under multi-factor coupling.

2 Overview of the study area and data sources

2.1 Study area

Qingdao was selected as the study area because of its distinct geographical advantages, as shown in Figure 1. Located in the southern part of the Shandong Peninsula, Qingdao borders Yantai, Weifang, and Rizhao to the north, west, and south, respectively, and faces the Yellow Sea to the east. The city covers a total area of 11,300 km² and has approximately 760 km of mainland coastline, of which about 211 km are natural coastlines. Qingdao has numerous offshore islands within its administrative jurisdiction, including seven inhabited and 113 uninhabited islands. The region features a temperate monsoon climate, with an average annual precipitation of 637.3 mm in 2023. Three major mountain systems shape the city’s topography: the Laoshan Mountains in the southeast, with a peak elevation of 1,133 m; the Dazeshan Mountains in the north, with a peak elevation of 736.7 m; and the Jiaonan mountain group in the southwest, which includes Dazhushan and Xiaozhushan. The Qingdao coastal zone is a representative bedrock bay-type coastline in northern China, characterized by a highly indented shoreline with alternating capes and bays. The terrain is dominated by hills and plains, and the region supports diverse ecosystems, including coastal wetlands, tidal flats, and estuaries. More than ten rivers, including the Dagu River, Yang River, and Baisha River, flow into Jiaozhou Bay, forming a complex network of land-sea material cycling and

TABLE 1 Data sources and description.

Data description	Data sources	Spatial resolution	Year	DOI/URL	Preprocessing
Administrative boundary	Tianditu	1:250,000	2024	http://www.tianditu.gov.cn	Projection; Validate Topology; Clip
Digital Elevation Mode (DEM)	GEBCO Compilation Group (2023)	15 arc-second	2023	DOI:10.5285/f98b053b-0cbc-6c23-e053-6c86abc0af7b	Projection; Validate Topology; Clip
Road Waters	OpenStreetMap	Not applicable (vector data)	2015 2020	https://www.openstreetmap.org	Validate Topology; Accuracy assessment; Projection; Resample; Clip
Land cover	The 30 m annual land cover datasets and its dynamics in China from 1990 to 2020 (Yang and Huang, 2021)	30 m	2010 2015 2020	https://doi.org/10.5281/zenodo.5816591	Accuracy Assessment; Clip
Population	WorldPop	100 m	2015 2020	DOI:10.5258/SOTON/WP00839	Resample; Projection; Clip
GDP	Scientific Data	1000m	2015 2020	https://doi.org/10.1038/s41597-025-04487-x	Resample; Projection; Clip

energy exchange. These systems contain several important sedimentary carbon pools that play a crucial role in the regional carbon cycle.

2.2 Data sources

The data used in this study include four major categories: basic geographic information, land use, socio-economic data, and natural environmental variables. All datasets were uniformly preprocessed to ensure spatial consistency and methodological compatibility. The Population and GDP driving factors were derived from global gridded datasets with annual continuity. The positional accuracy of OSM vector data varies spatially and depends on local mapping practices and source imagery. This study directly adopted the gridded datasets for 2015 and 2020 as driving factor inputs for land-use simulation, without requiring temporal interpolation. All raster layers were uniformly clipped and reprojected to match the spatial resolution of the land-use data, ensuring consistency across temporal and spatial scales. Using the Project Raster tool in ArcGIS 10.8, the coordinate systems of the six driving factor datasets were unified to WGS_1984_Albers. Detailed data sources and descriptions are provided in Table 1.

3 Research methods

This study establishes a technical framework that integrates land-use change analysis, carbon storage estimation, multi-model coupling and validation, and the quantitative assessment of driving mechanisms. By combining land-use transition matrices with the InVEST and PLUS models, this study conducts a systematic investigation of the spatiotemporal evolution and driving mechanisms of carbon storage in the Qingdao coastal zone and evaluates how these spatial dynamics inform and align with coastal-zone planning.

3.1 Land-use transition matrix

The land-use transition matrix is a fundamental method for quantifying the direction, magnitude, and intensity of land-use conversions over a given period, and it clearly reveals the source-sink transformation relationships among different land-use categories. The core principle is to represent the correspondence between land-use types at the beginning and end of a given period in matrix form, thereby providing a basis for attributing subsequent changes in carbon storage. The formula for constructing the land-use transition matrix based on land-use conditions in each period is as follows (Equation 1):

$$S_{ij} = \begin{bmatrix} S_{11} & S_{12} & \dots & S_{1n} \\ S_{21} & S_{22} & \dots & S_{2n} \\ \vdots & \vdots & \vdots & \vdots \\ S_{n1} & S_{n2} & \dots & S_{nn} \end{bmatrix} \quad (1)$$

where S represents the area, n represents the total number of land-use types, i refers to the land-use type at the beginning of the study, and j is the land-use type at the end of the study period (Chen et al., 2024).

3.2 InVEST model

The Carbon Storage and Sequestration (CSS) module of the InVEST model is based on ecosystem carbon pool accounting principles. By integrating carbon density data for different land-use types, it enables spatially explicit estimation of regional carbon storage and offers the advantages of clearly defined physical parameters and highly visualized results. This study uses carbon density data from four pools, including aboveground biomass, belowground biomass, soil carbon, and dead organic matter. Combined with land-use data for each period, the carbon densities of the four pools are applied to calculate the total carbon storage of the study area. The calculation formula is as follows (Equation 2):

TABLE 2 Carbon density values for different land-use types (t-ha⁻¹).

LULC	lucode	C _{above}	C _{below}	C _{soil}	C _{dead}	Study area	References
Farm land	1	9.84	8.79	34.57	0.31	Coastal areas; Shandong Province; The Yellow River Delta	Xu (Xu et al., 2018); Lyu (Lyu and Li, 2025); Xu (Xu et al., 2025); Wang (Wang et al., 2024); Zheng (Zheng and Zheng, 2023); Zhu (Zhu et al., 2022)
Forest	2	35.2	6.59	92.95	3.13		
Grassland	3	12.09	13.18	68.76	1.2		
Waters	4	0.4	0.2	0	0		
Bare land	5	0.5	0	19.38	0		
Architecture	6	0.87	0	20.05	0		

$$C_{total} = C_{above} + C_{below} + C_{soil} + C_{dead} \quad (2)$$

where C_{total} , C_{above} , C_{below} , C_{soil} , C_{dead} represent the total carbon storage, aboveground carbon pool, belowground carbon pool, soil organic carbon pool, and dead organic matter carbon pool, respectively (Sharp et al., 2018).

Based on the Chinese Terrestrial Ecosystem Carbon Density Dataset from the National Ecosystem Science Data Center, this study prioritizes carbon density values for each land-use type from regions with latitudinal positions and ecological backgrounds similar to those of the study area. Additional references were integrated from related studies, including research on forest belowground carbon in China, forest soil organic carbon (SOC) in eastern China, the spatiotemporal characteristics of carbon storage in ecological land across coastal areas of Shandong Province, the spatial distribution of soil organic carbon density in the Shandong Peninsula, cropland SOC in Shandong Province, and empirical carbon density data from typical regions of Shandong, such as the Yihe River Basin and the Yellow River Delta. In the absence of direct observational data, dead organic carbon was estimated using a commonly adopted ratio from the literature, in which the ratio of dead organic carbon to aboveground biomass carbon is approximately 1:10 (Delaney et al., 1998). On this basis, a carbon density dataset suitable for the study area was constructed. Table 2 summarizes the carbon density parameters assigned to each LULC class as inputs to the InVEST carbon storage model. Each LULC class was mapped to the four carbon pools (AGB, BGB, SOC, and Dead) in accordance with IPCC carbon stock accounting principles.

3.3 PLUS model

The PLUS model integrates the Land Expansion Analysis Strategy (LEAS) with a cellular automata model based on multiple random patch seeds (CARS) to achieve high-precision simulation of land-use change. Its core advantage lies in quantifying the contributions of multiple driving factors to the expansion of different land-use types using Random Forest Classification (RFC) (Liang et al., 2021). Meanwhile, the patch seed generation mechanism improves the simulation of spatial patterns, making the model more suitable than traditional approaches for simulating land-use change in complex coastal regions (Zhu et al., 2025). The LEAS module extracts expansion pixels of each land-use type from historical land-use changes as positive samples and randomly selects an equal number of negative samples from unchanged areas to train the Random Forest classifier.

Considering the natural geographic characteristics and the intensity of human activities in Qingdao's coastal zone, six core driving factors were selected to represent both natural and anthropogenic dimensions. The driving factors were selected based on relevance, data availability, representativeness, spatial heterogeneity, coverage of natural and socio-economic conditions, and interpretability of results, ensuring the reliability of the simulation. Using the 2020 dataset as the prediction scenario, the driving factor dataset and the baseline land-use data were input into the LEAS module. The Random Forest algorithm was then applied to calculate the contribution weights of each driving factor to the expansion of Farm land, Forest, Grassland, and Architecture, thereby identifying the dominant drivers of land-use change. Based on the expansion probability maps generated by the LEAS module, the CARS module was used to simulate the spatial land-use pattern in 2020. Model performance was evaluated using the Kappa coefficient and the Figure of Merit (FoM). A Kappa value ≥ 0.75 indicates good agreement between the simulated results and the observed data and supports the suitability of the model for subsequent scenario simulations. After data preprocessing, including standardization and raster harmonization, the 2010 land-use dataset was used as the baseline, and six driving factors, including DEM, Slope, GDP, Population, Road, and Water proximity, were adopted as input variables. The RFC module was then used to generate the spatial expansion potential of each land-use type for 2020.

In the LEAS module, the key parameters of the RFC were configured as follows: the sampling rate was set to 0.01, the number of regression trees was set to 10, the number of threads was set to 5, and the maximum number of features was defined as the number of driving factors. The training performance of the RFC was evaluated using the root mean square error (RMSE), with values ranging from 0 to 1. A smaller RMSE indicates better model fitting. In this study, the RMSE values for different land-use types ranged from 0.12 to 0.18, indicating a relatively low level of error. This suggests that the constructed transition probability models exhibit good explanatory power and reliability and are suitable for subsequent land-use change simulations. The land-use transition matrix for each land-use type is shown in Table 3, where "1" indicates that conversion is allowed and "0" indicates that conversion is not permitted. The columns represent the baseline land-use types, and the rows represent the target land-use types. In this study, four conversion constraints were applied: Forest cannot be converted to Waters; Waters cannot be converted to Forest or Architecture; and Architecture cannot be converted to Waters.

TABLE 3 Land-use conversion constraint matrix.

LULC	Farm land	Forest	Grassland	Waters	Bare land	Architecture
Farm land	1	1	1	1	1	1
Forest	1	1	1	0	1	1
Grassland	1	1	1	1	1	1
Waters	1	0	1	1	1	0
Bare land	1	1	1	1	1	1
Architecture	1	1	1	0	1	1

In the CARS module, all parameters were set to the default values of the PLUS model: the Neighborhood radius was 3, the Decay threshold was 0.5, the Diffusion coefficient was 0.1, and the Random patch seed probability was 0.0001. The number of threads was consistent with the LEAS module and was set to 5. The expansion weights for different land-use types were manually assigned to reflect their heterogeneity in spatial evolution. Based on the land expansion maps, the proportion of each land-use type's expansion area relative to the total land expansion was calculated to determine the neighborhood weight for each type. The weight values corresponding to higher simulation accuracy were selected, with values ranging from 0 to 1. When the neighborhood factor weights were calculated using deviation standardization (Weight-1), zero values appeared, and the expansion capacity of Farm land became unreasonable. Therefore, the neighborhood weights proposed by Wang Bo (Wang, 2023) (Weight-2) were adopted as a reference. A comparison between the two weighting schemes is shown in Table 4.

4 Results and analysis

4.1 Changes in land-use types

Based on the preprocessed CLCD dataset and following boundary clipping and classification standard harmonization for the Qingdao coastal zone, six land-use categories were ultimately defined for the study area: Farm land, Forest, Grassland, Waters, Bare land, and Architecture.

The structural changes in land-use types across 2010, 2015, and 2020 are shown in Figure 2. Farm land remained the dominant land-use type throughout the study period, accounting for more than 65% of the total area. The study area exhibited a clear “dual-dominant” pattern, with Farm land and Architecture together representing more than 90% of the total area, indicating their primary role in shaping regional ecosystem structure and carbon-cycle processes. During 2010–2020, the proportion of Farm land decreased from 69% to approximately 66%, while Architecture increased from 23% to 27%,

representing the most significant expansion among all land-use types. Changes in other categories were relatively limited, with a slight increase in Forest, a minor decline in Grassland, and small fluctuations in Waters, which showed an overall decreasing trend.

4.2 Changes in carbon storage

Total carbon storage in the study area was 5.3174×10^7 t in 2010, declined to 5.3055×10^7 t in 2015, and further decreased to 5.2749×10^7 t in 2020. From a temporal perspective, total carbon storage in Qingdao's coastal zone exhibited a trend of “continuous but gradual decline” during 2010–2020, although the rates of change varied significantly across different stages. The average annual decrease was approximately 2.38×10^4 t during 2010–2015, while it increased to 6.12×10^4 t during 2015–2020, which is about 2.6 times that of the previous stage. This latter period represents the steepest decline in carbon storage throughout the study interval. Around 2015 marked a critical turning point in carbon storage change, as the study area shifted from a phase of “slow decline” to one of “accelerated decrease.” This transition closely coincided with the reduction in Farm land and Grassland, the expansion of port-related industrial land, and the acceleration of urban development, indicating that rapid urbanization is a key driver of the intensified decline in carbon storage.

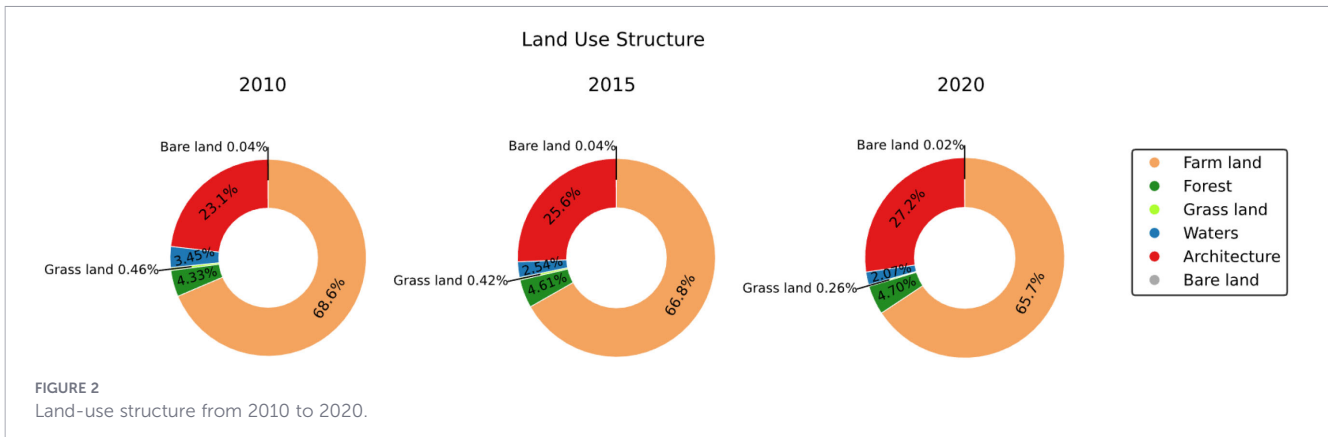
4.3 PLUS model simulation and spatial characteristics

The simulation results indicate that the expansion potential of different land-use types exhibits pronounced spatial heterogeneity (Figure 3). Farm land, Forest, Grassland, and Architecture show clear expansion tendencies, whereas Waters and Bare land exhibit relatively limited expansion potential due to their smaller and more fragmented distributions. In terms of spatial patterns, the expansion of Architecture and Forest is more clustered, while that of Farm land and Grassland is more dispersed.

In this study, the land-use data for 2010 and 2015 were used as baseline periods, and a Markov chain model was applied to predict land-use transition probabilities. These probabilities were then coupled with the CARS module of the PLUS model to construct a simulation

TABLE 4 Neighborhood weights.

	Farm land	Forest	Grassland	Waters	Bare land	Architecture
Weight-1	0.73	0.11	0.02	0.36	0	1
Weight-2	0.176	0.062	0.02	0.238	0.491	0.012



framework that integrates transition probabilities with spatial pattern processes to predict the 2020 land-use distribution of Qingdao’s coastal zone. The simulated results were validated against the observed 2020 land-use data to assess the consistency between the model outputs and the observed conditions. The calculated Kappa coefficient between the simulated and observed results was 0.793948 ($Kappa \geq 0.75$), and the FoM value was 0.168, both meeting the accuracy requirements. These results indicate a high level of consistency between the simulated and observed land-use quantity structures. The simulated and observed land-use patterns are shown in Figures 4a, b. The discrepancies between the simulation and the observed distribution are mainly concentrated in two key land-use types. First, in areas surrounding major Waters patches, some regions were simulated as converting to Farm land. Second, the simulated expansion of Architecture along the Jiaozhou Bay coastline is slightly smaller than observed, which is associated with the accelerated development of port-related industrial land during this period and is not fully captured by the model. Both types of discrepancies represent reasonable deviations arising from differences between policy timing and model parameterization and do not affect the overall validity of the spatial pattern simulation.

The 2020 land-use data simulated by the PLUS model were input into the CSS module of the InVEST model, yielding a regional carbon storage estimate of 5.2628×10^7 t. Compared with the observed carbon storage, the relative error was 0.23%, which falls within an acceptable error range ($\pm 1\%$). This result indicates that the PLUS model can effectively capture the driving effects of land-use structure evolution on carbon storage, and that the relationships between the simulated land-use patterns and carbon storage responses are reliable. Using these results to analyze the driving factors of carbon storage change in Qingdao’s coastal zone is therefore reasonable and can provide scientific support for future scenario-based carbon storage projections and coastal planning decision-making.

5 Discussion

5.1 Analysis of land-use transition characteristics and driving mechanisms

From 2010 to 2020, the proportion of Architecture in Qingdao’s coastal zone increased continuously, reflecting pronounced spatial

expansion driven by urbanization and port-oriented development. According to the land-use transition matrix (Figure 5), the primary source of Architecture expansion was Farm land, highlighting the strong encroachment of urban growth on agricultural space. By contrast, the proportions of Forest and Waters remained generally stable (approximately 4–5% and 2–3%, respectively), while Grassland and Bare land accounted for only very small shares and had limited influence on the overall land-use structure. This pattern indicates that ecological protection policies and territorial spatial use controls have remained effective in imposing rigid constraints on core ecological land. Overall, land-use evolution in the study area exhibits a pattern characterized by the expansion of Architecture, the contraction of Farm land, and the general stability of ecological land, reflecting a spatial restructuring process under hierarchical regulation. From a system-evolution perspective, land-use change during 2010–2020 was dominated by the continuous and cumulative expansion of Architecture, primarily converted from Farm land, with smaller contributions from Grassland and Waters. Once converted, these areas rarely reverted, indicating clear irreversibility in the land-use transition process. By contrast, Farm land experienced continuous net losses. Although limited local compensation from Grassland or Forest occurred in some areas, it remained insufficient to offset the intensity of urban encroachment. The bidirectional conversion between Grassland and Forest, together with the stage-wise variations of Waters under the combined influence of natural fluctuations and engineering interventions, reveals the complex responses of ecosystems to the coupling of natural succession and human disturbance. Bare land mainly appears as a transitional state during the conversion of Farm land or Grassland to Architecture, reflecting the stage-wise succession of land-use types under rapid urbanization.

The carbon storage transition matrix was used to quantify the differences in carbon density before and after each land-use conversion pathway (ΔC), thereby enabling analysis of the response mechanisms of carbon storage to land-use change (Wei et al., 2023; Jia et al., 2022; Zhang et al., 2024). ΔC was used to represent the carbon effect of different land-use conversion pathways: $\Delta C > 0$ indicates carbon-gain transitions, whereas $\Delta C < 0$ indicates carbon-loss transitions. A larger absolute value of ΔC corresponds to a stronger carbon effect per unit area. The carbon storage transition matrices for each land-use type during 2010–2015 and 2015–2020 are shown in Tables 5 and 6, respectively.

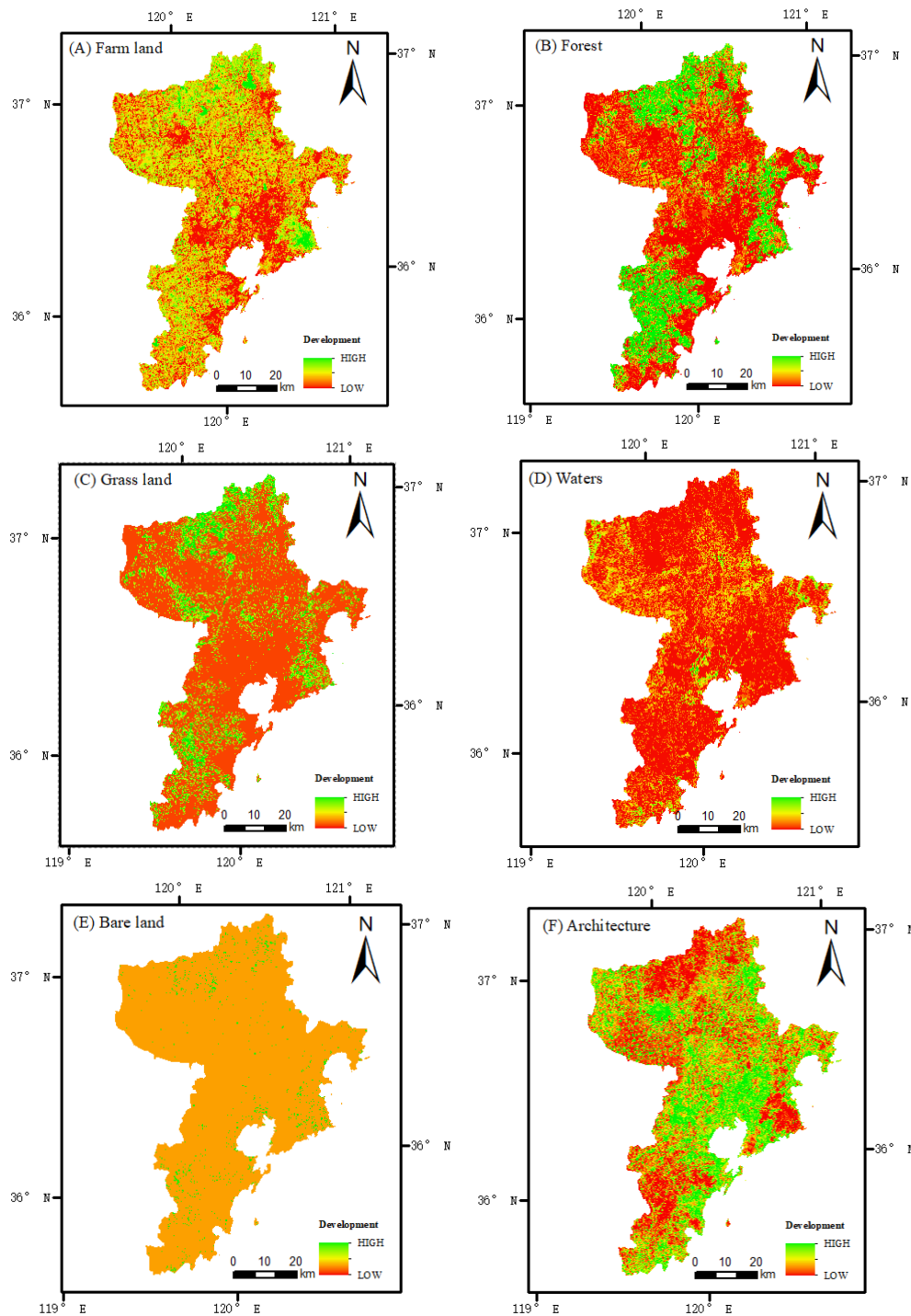


FIGURE 3 Development potential of each land-use type at the grid-cell level. (A) Farm land. (B) Forest. (C) Grass land. (D) Waters. (E) Bare land. (F)Architecture.

A comparison of the two transition matrices reveals a clear turning point in the carbon effects of land-use change around 2015 in Qingdao’s coastal zone. The ΔC values of carbon-loss pathways represented by the conversion of Farm land to Architecture decreased, while those of carbon-gain transitions, such as the conversion of Grassland to Forest increased. At the same time, carbon-loss pathways such as the conversion of Forest and Grassland to Farm land intensified after 2015, indicating that regional carbon storage dynamics are jointly driven by urban

expansion and production land expansion. Overall, the conversion of Farm land to Architecture represents the dominant source of carbon loss ($\Delta C = -12.623 \times 10^5$ t), whereas the conversion of Farm land to Forest constitutes the most important carbon-gain pathway ($\Delta C = 7.622 \times 10^5$ t). Spatially, carbon storage hotspots are mainly concentrated in the urban core and the urban expansion belt along Jiaozhou Bay, while cold spots are distributed in the Laoshan area and the forest-dominated northern hilly regions, indicating that the carbon storage pattern is

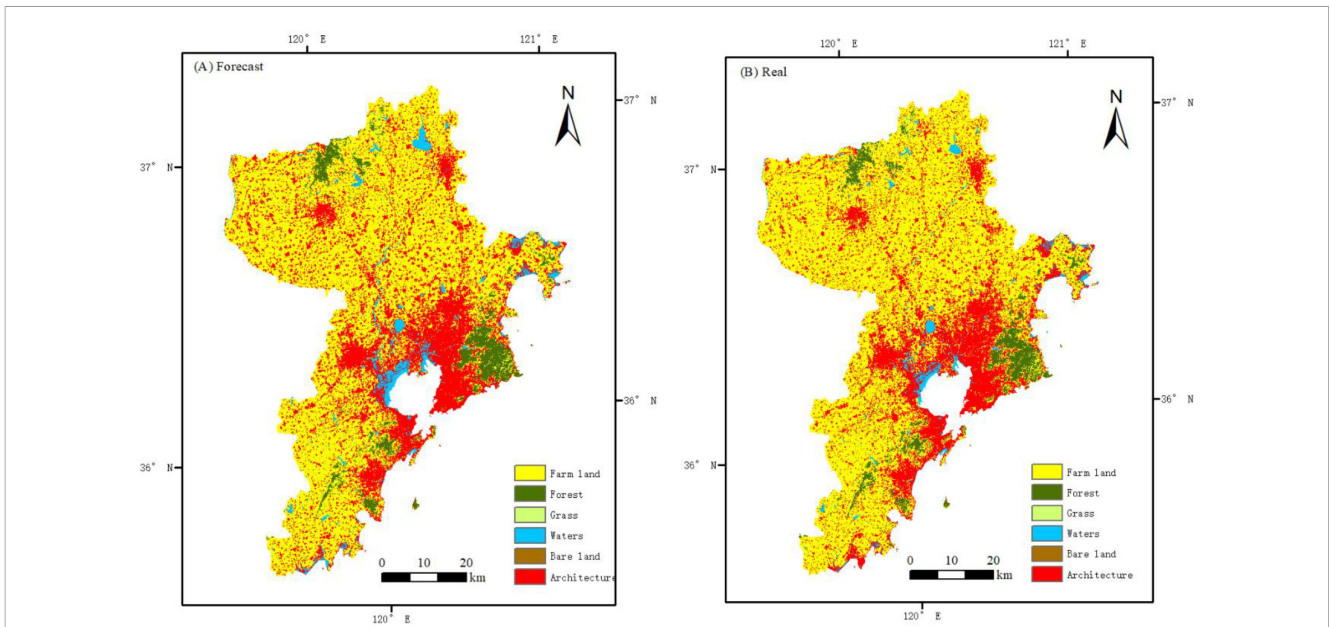


FIGURE 4 Comparison between forecast and real land-use patterns. (A) Forecast. (B) Real.

primarily driven by the spatial clustering of high-intensity land-use conversion pathways.

5.2 Analysis of driving factors behind carbon-storage change

This study selected six driving factors, including DEM, Road, GDP, Slope, Population, and Water, to analyze land-use change

drivers. Based on the land-use data from 2010 and 2015, land-use changes in 2020 were predicted, and the contribution of each driving factor was examined to identify the dominant drivers for each land-use type. The contributions of each driving factor to the expansion of different land-use types, as calculated by the LEAS module, are presented in Table 7. The effects of the driving factors exhibit pronounced land-use-type-specific differences.

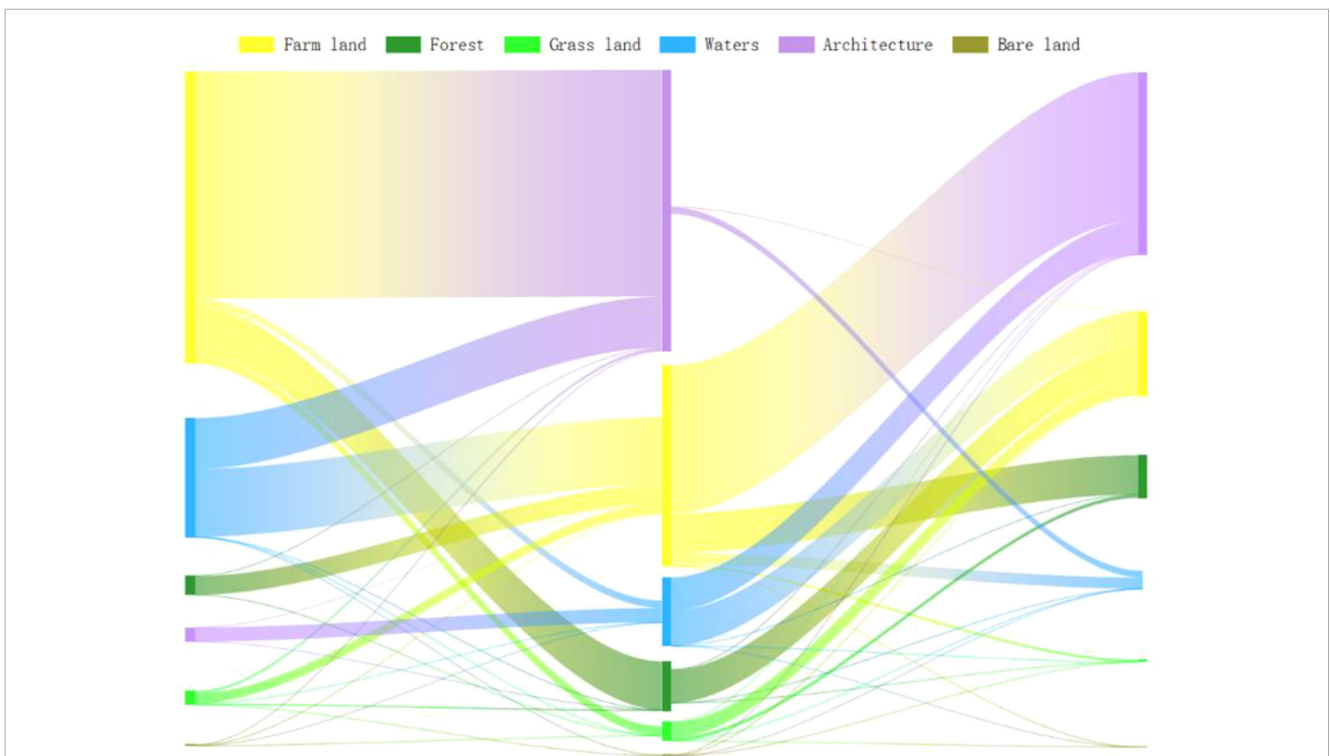


FIGURE 5 Land-use transition matrix.

TABLE 5 Carbon storage transition matrix among land-use types during 2010–2015. (unit: 10⁵ t).

LULC	Farm land	Forest	Grassland	Waters	Bare land	Architecture
Farm land	0.000	4.208	0.400	-0.413	0.000	-7.635
Forest	-1.644	0.000	-0.001	0.000	0.000	-0.077
Grassland	-0.420	0.060	0.000	-0.032	-0.009	-0.192
Waters	3.708	0.015	0.002	0.000	0.021	1.070
Bare land	0.019	0.000	0.017	-0.002	0.000	0.001
Architecture	0.007	0.000	0.000	-0.299	0.000	0.000

(1) For the four ecological land types, including Farm land, Forest, Grassland, and Waters, natural factors such as DEM, Slope, and Water proximity exert strong influences, indicating that terrain and hydrological conditions play dominant roles in shaping these land-use categories. Farm land expansion is mainly concentrated in the central part of the study area, where population density is higher, terrain is relatively flat, and irrigation access is convenient. This pattern is consistent with agriculture’s dependence on stable topography and water availability. Forest expansion is primarily influenced by terrain, population density, and water availability, reflecting the combined effects of natural processes and human interventions and its role as a carbon-sink-dominant land type. Mountainous and hilly areas such as Laoshan and Xiaozhushan, characterized by low human disturbance and compliance with ecological redline protection requirements, have become priority zones for natural forest recovery and afforestation, demonstrating the positive role of targeted human intervention in enhancing carbon sinks. Grassland is most strongly influenced by DEM, with a contribution value of 0.35, suggesting that higher-elevation and less-developed areas are more conducive to grassland expansion. The drivers of water-body expansion exhibit a clear natural–anthropogenic duality. From a natural perspective, DEM and water adjacency are the dominant factors, maintaining spatial continuity with river–lake systems. In addition, the contributions of population and GDP indicate that artificial water-body construction, water-environment management, and hydraulic engineering also significantly influence water-area dynamics, resulting in a combined natural–engineering expansion pattern.

(2) For Architecture and Bare land, socio-economic factors serve as the primary drivers. Architecture is particularly sensitive to population, with a contribution value of 0.29, indicating that population agglomeration and urbanization are the main forces behind the outward expansion of urban boundaries. GDP and road proximity further indicate that transportation accessibility and

economic development levels strongly influence the growth of construction land, with expansion tending toward areas with higher accessibility and more favorable terrain. Bare-land expansion is driven primarily by population factors, whose contribution far exceeds that of other variables, suggesting that bare land represents a transitional land state associated with rapid urbanization. As a carbon-source-dominant land type, architecture also reflects the strong capacity of human activities to reshape natural terrain, as evidenced by the contribution of DEM. This finding supports the conclusion that urbanization and port-oriented industrial development in the Qingdao coastal zone generate rigid demand for construction land, driving the expansion of residential, industrial, and port-related facilities and directly encroaching on farm land, grassland, and other carbon-sink land types.

By integrating the land-use transition matrix with carbon storage evolution results, the transmission mechanism of driving factors on carbon storage change can be summarized as a “dual-path coupling” process. The direct pathway operates through natural factors that regulate carbon density by influencing the distribution and productivity of carbon-sink land, such as forest and wetlands. The indirect pathway operates through anthropogenic factors, including GDP and population, which drive land-use conversions and change the area proportions of carbon-sink and carbon-source land, thereby inducing variations in total carbon storage.

5.3 Spatial heterogeneity of carbon storage and its planning adaptability

From 2010 to 2020, the spatial distribution of carbon storage in Qingdao’s coastal zone exhibited a pronounced heterogeneous pattern, characterized by clustered high-value zones, contiguous medium-value zones, and radially distributed low-value zones

TABLE 6 Carbon storage transition matrix among land-use types during 2015–2020. (unit: 10⁵ t).

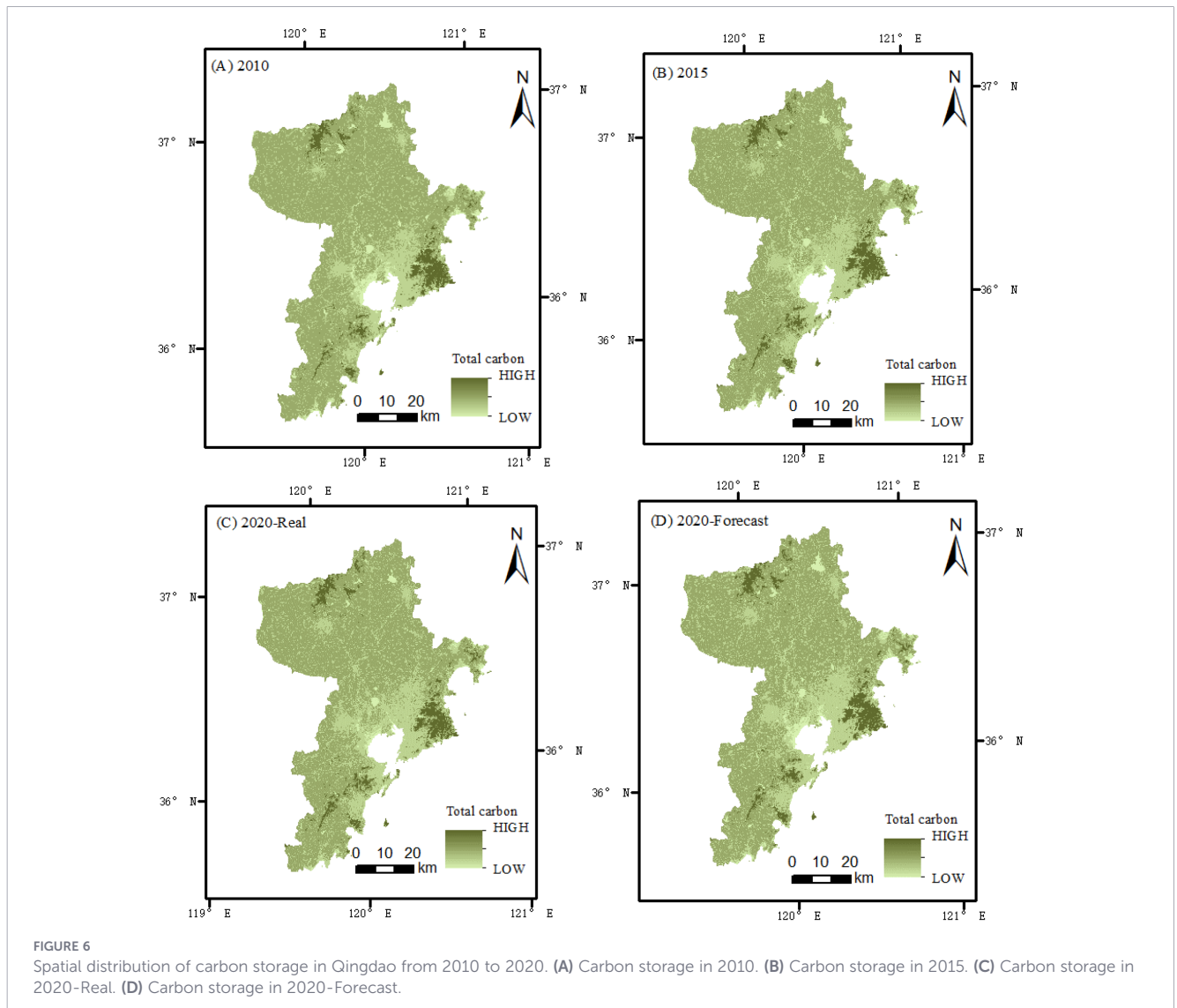
LULC	Farm land	Forest	Grassland	Waters	Bare land	Architecture
Farm land	0.000	3.414	0.103	-0.620	0.000	-4.988
Forest	-2.896	0.000	-0.006	-0.001	0.000	-0.040
Grassland	-0.649	0.158	0.000	-0.001	-0.007	-0.060
Waters	1.916	0.021	0.001	0.000	0.005	0.696
Bare land	0.025	0.000	0.013	-0.005	0.000	0.001
Architecture	0.004	0.000	0.000	-0.142	0.000	0.000

TABLE 7 Contribution of each driving factor to the expansion of different land-use types.

LULC	DEM	Road	GDP	Slope	Population	Water
Farm land	0.31	0.14	0.11	0.03	0.18	0.22
Forest	0.25	0.14	0.13	0.04	0.22	0.22
Grassland	0.35	0.18	0.19	0.03	0.07	0.17
Waters	0.25	0.13	0.15	0.05	0.20	0.23
Bare land	0.11	0.08	0.05	0.02	0.66	0.08
Architecture	0.26	0.13	0.12	0.03	0.29	0.17

(Figure 6). High carbon storage areas are clustered in the northern Laoshan Mountains, the Xiaozhushan Forest Park in the southeast, and the Yanghe River estuary wetland reserve in the southwest. These regions are dominated by forest and wetlands (accounting for more than 85%), exhibit high vegetation coverage, and are constrained by ecological protection red lines with low levels of human disturbance, making them the core carbon sink areas of the study region. Medium-value zones are mainly distributed across the central plains dominated by farmland, interspersed

with architecture and waters. Low carbon storage zones are concentrated around the Jiaozhou Bay coastline and are dominated by architecture, with carbon storage decreasing radially from Jiaozhou Bay. From a temporal perspective, the overall spatial pattern remained relatively stable from 2010 to 2020; meanwhile, low-value zones expanded markedly along urban fringes, and some high-value patches became increasingly fragmented. This suggests that urbanization and the expansion of architecture are important drivers of carbon storage decline.



By integrating the land-use and carbon storage transition pathway results, a clear structural turning point in carbon effects is observed around 2015 in the study area. Expansion-driven pathways, such as the conversion of farm land to architecture, became markedly less intense after 2015, and their negative carbon effects were significantly weakened. At the same time, pathways such as the conversion of forest and grassland to farm land intensified, resulting in more pronounced carbon losses. This turning point shows strong temporal consistency with the implementation milestones of multiple spatial regulation and ecological protection policies in Qingdao. The Three-Year Action Plan for Building a National Ecological City in Qingdao (2014–2016) and the Outline of the 13th Five-Year Plan for National Economic and Social Development of Qingdao (2016–2020) explicitly designated ecological protection red lines, permanent basic farmland, and urban growth boundaries as rigid constraints, thereby strengthening controls on the disorderly expansion of architecture. Meanwhile, under the constraints of the cultivated land balance policy and the permanent basic farmland protection system, some ecological land was converted to farm land to meet replenishment requirements, which in turn exacerbated localized carbon losses. In addition, the implementation of the Qingdao Bay Protection and Governance Plan in 2017 and the Qingdao Wetland Protection Regulations in 2018 exerted guiding effects on conversion pathways between farm land and waters. Overall, the carbon-effect turning point around 2015 is more likely the combined result of multiple spatial regulation and ecological protection policies, which reshaped both the pathways and magnitudes of land-use transitions.

The spatial heterogeneity of carbon storage in the study area is mainly influenced by the combined effects of topography, land-use structure, and vegetation cover. From 2010 to 2020, the land-use structure exhibited a pattern characterized by a reduction in farm land, an expansion of architecture, a slight increase in forest, and an overall contraction of ecological land. The carbon losses caused by the expansion of architecture and the decline of farm land could not be offset by the modest increase in forest, resulting in an overall decrease in regional carbon storage. This spatial heterogeneity provides clear guidance for coastal spatial planning. High carbon storage zones should prevent patch fragmentation and strengthen ecological connectivity, low carbon storage zones should strictly control construction intensity and shoreline development, and medium carbon storage zones can enhance carbon sink potential by increasing soil organic carbon and promoting ecological agricultural practices, thereby facilitating the coordinated optimization of carbon sink functions and territorial spatial patterns. The spatial heterogeneity observed in the study area is consistent with the general patterns of carbon storage distribution in eastern coastal cities of China. Due to Qingdao's bedrock bay geomorphology and port-oriented industrial structure, its high carbon storage zones are subject to stronger topographic constraints, while the radiating effects of low carbon storage zones are more pronounced. This distinction provides a useful reference for spatial planning in similar coastal regions.

5.4 Limitations and future perspectives

Although this study systematically reveals the spatiotemporal evolution of land-use patterns and carbon storage in Qingdao's

coastal zone through the coupled InVEST–PLUS model, certain limitations remain. The InVEST model estimates carbon storage using fixed carbon density parameters and does not fully account for the effects of vegetation growth dynamics, climate change, and human disturbances on carbon sink processes, which may introduce static biases in the estimates for some local areas. Secondly, future scenario simulations using the PLUS model are strongly influenced by the selection of driving factors and socio-economic assumptions, and the associated uncertainties in model outputs still require further evaluation through multi-scenario comparisons and sensitivity analyses. Moreover, the temporal scale of this study is limited to a five-year projection horizon and therefore does not capture seasonal or short-term fluctuations in carbon sinks.

Future research may be advanced in the following three aspects. First, by incorporating zoned constraints and multi-scenario land-use simulations, uncertainties arising from LULC classification, carbon density parameters, and PLUS scenario simulations can be explicitly integrated into the carbon accounting framework and combined with quantifiable human-activity control scenarios. By coupling scenario simulations with parameter sensitivity analyses, an integrated carbon storage assessment system with a process–response–feedback structure can be developed. Second, multi-source remote sensing data, ecological surveys, and process-based models can be integrated to enable dynamic updating and more refined representation of carbon storage estimates, while incorporating socio-economic and ecological co-driving mechanisms to characterize the coupled relationships among human activities, land use, and carbon storage responses. Third, in conjunction with coastal territorial spatial planning practices, a carbon sink zoning regulation and restoration priority identification mechanism based on ecological security patterns should be further developed. By controlling coastal construction intensity, coordinating blue-carbon and green-carbon spaces, and strengthening dynamic monitoring of high-value areas, this approach can support regional low-carbon transitions and territorial spatial governance.

6 Conclusions and recommendations

This study employs a coupled InVEST–PLUS multi-model framework to systematically analyze the spatiotemporal reconstruction of land use, the evolution of carbon storage, and the underlying driving mechanisms in Qingdao's coastal zone from 2010 to 2020, and to clarify the central guiding role of carbon sink dynamics in coastal spatial planning. By integrating changes in land-use proportions with the characteristics of carbon storage transition pathways, this study identifies the expansion of Architecture and the contraction of ecological land as the core mechanisms driving the decline in carbon storage in Qingdao's coastal zone. High carbon-loss pathways, represented by the conversion of Farm land, Grassland, and Waters into Architecture, are spatially concentrated in coastal development belts, port-related industrial zones, and urban expansion fringes, and exert persistent negative impacts on the regional carbon sink pattern.

Meanwhile, the conversion of Forest and Grassland to Farm land and other production land showed an increasing trend during certain periods, further weakening the ecosystem's carbon storage function. These findings indicate that carbon storage change in the study area is not driven by a single land-use transition, but by the spatial superposition of multiple high-intensity conversion pathways. Future territorial and coastal detailed spatial planning should therefore treat high carbon-effect conversion pathways as primary regulatory targets. The specific policy recommendations are outlined below.

1. Carbon-loss hotspots and carbon-sink cold spots should be designated as first-priority units for spatial regulation. In carbon-loss hotspot areas, including the Jiaozhou Bay coastline, port-oriented industrial belts, and urban expansion fringes, the conversion of Farm land, wetlands, and Grassland to Architecture should be strictly restricted. In carbon-sink cold-spot areas, such as Laoshan, Xiaozhushan, and estuarine wetland zones, ecological red-line controls and restoration measures should be prioritized.
2. Carbon change intensity per unit area ($\Delta C/\text{ha}$) can be adopted as an important threshold indicator for land-use admittance and zoned regulation, helping to establish a territorial spatial governance framework that is constrained by carbon effects. A carbon sink compensation mechanism can be incorporated into cultivated land occupation-compensation balance policies and land-use regulation, thereby quantitatively coordinating development demands with ecological security and providing decision support for Qingdao's low-carbon transition.
3. A dynamic monitoring system that integrates multi-source remote sensing, field surveys, and model simulations can be established to enable long-term tracking and assessment of high carbon storage zones and key conversion corridors. Land-use and ecological status information should be updated regularly, and medium-carbon-storage areas such as Farm land should be incorporated into "carbon sink function protection zones" for differentiated management, thereby ensuring the stability of regional carbon storage and the sustained functioning of ecological barriers.

Data availability statement

The original contributions presented in the study are included in the article/supplementary material. Further inquiries can be directed to the corresponding author.

Author contributions

CX: Conceptualization, Investigation, Methodology, Software, Validation, Visualization, Writing – original draft, Writing – review & editing. CW: Conceptualization, Formal Analysis, Funding

acquisition, Investigation, Methodology, Resources, Writing – original draft, Writing – review & editing. DL: Funding acquisition, Methodology, Resources, Writing – original draft. ZZ: Methodology, Resources, Writing – original draft. YL: Funding acquisition, Methodology, Resources, Writing – original draft. ZL: Software, Validation, Visualization, Writing – original draft.

Funding

The author(s) declared that financial support was received for this work and/or its publication. National Natural Science Foundation (42376228); Natural Science Foundation Project of Shandong (ZR2025MS542); The National Key Research and Development Program of China (2022YFC3800801).

Acknowledgments

The authors extend their sincere gratitude to the organizations and individuals who contributed to this research. We thank the various data-development teams for providing open-access datasets that made this study possible. The authors also appreciate the constructive suggestions from colleagues and the support of the laboratory team during data processing and model validation.

Conflict of interest

The author(s) declared that this work was conducted in the absence of any commercial or financial relationships that could be construed as a potential conflict of interest.

Generative AI statement

The author(s) declared that generative AI was not used in the creation of this manuscript.

Any alternative text (alt text) provided alongside figures in this article has been generated by Frontiers with the support of artificial intelligence and reasonable efforts have been made to ensure accuracy, including review by the authors wherever possible. If you identify any issues, please contact us.

Publisher's note

All claims expressed in this article are solely those of the authors and do not necessarily represent those of their affiliated organizations, or those of the publisher, the editors and the reviewers. Any product that may be evaluated in this article, or claim that may be made by its manufacturer, is not guaranteed or endorsed by the publisher.

References

- Chen, S., Wang, X., Qiang, Y., and Lin, Q. (2024). Spatial-temporal evolution and land use transition of rural settlements in mountainous counties. *Environ. Sci. Eur.* 36, 38. doi: 10.1186/s12302-024-00868-y
- Cramer, W., Guiot, J., Fader, M., Garrabou, J., Gattuso, J.-P., Iglesias, A., et al. (2018). Climate change and interconnected risks to sustainable development in the Mediterranean. *Nat. Clim. Change* 8, 972–980. doi: 10.1038/s41558-018-0299-2
- Delaney, M., Brown, S., Lugo, A. E., Torres-Lezama, A., and Quintero, N. B. (1998). The quantity and turnover of dead wood in permanent forest plots in six life zones of Venezuela. *Biotropica* 30, 2–11. doi: 10.1111/j.1744-7429.1998.tb00364.x
- Duan, X., Yin, P., He, X., Chen, B., Cao, K., and Tong, G. (2025). Unraveling nonlinear interactions: A DPSIR-based conceptual model for synergistic impacts of climate change and human activities on coastal blue carbon ecosystems. *Global Change Biol.* 31, e70432. doi: 10.1111/gcb.70432
- Dyballa, K. E., Steger, K., Walsh, R. G., Smart, D. R., Gardali, T., and Seavy, N. E. (2019). Optimizing carbon storage and biodiversity co-benefits in reforested riparian zones. *J. Appl. Ecol.* 56, 343–353. doi: 10.1111/1365-2664.13272
- Hou, X., Yin, P., Ding, X., Zhang, Y., and Bi, S. (2012). Carbon storage capacity in the Daguhe wetland, Jiaozhou Bay of Qingdao. *Mar. Geology Front.* 28, 17–26. doi: 10.16028/j.1009-2722.2012.11.009
- Hou, Y., Wen, D., Wang, Z., Zhang, X., and Lou, Y. (2025). Spatiotemporal evolution and multi-scenario prediction of carbon storage in Dongting Lake Basin based on PLUS-InVEST model. *Environ. Sci.* 46, 6487–6500. doi: 10.13227/j.hjck.202410174
- Jia, P., Huang, W., Zhang, Z., Cheng, J., and Xiao, Y. (2022). The carbon sink of mangrove ecological restoration between 1988–2020 in Qinglan Bay, Hainan Island, China. *Forests* 13, 1547. doi: 10.3390/f13101547
- Lai, L., Huang, X., Yang, H., Chuai, X., Zhang, M., Zhong, T., et al. (2016). Carbon emissions from land-use change and management in China between 1990 and 2010. *Sci. Adv.* 2, e1601063. doi: 10.1126/sciadv.1601063
- Liang, X., Guan, Q., Clarke, K. C., Liu, S., Wang, B., and Yao, Y. (2021). Understanding the drivers of sustainable land expansion using a patch-generating land use simulation (PLUS) model: A case study in Wuhan, China. *Comput. Environ. Urban Syst.* 85, 101569. doi: 10.1016/j.compenurbysys.2020.101569
- Liu, X., Liang, X., Li, X., Xu, X., Ou, J., Chen, Y., et al. (2017). A future land use simulation model (FLUS) for simulating multiple land use scenarios by coupling human and natural effects. *Landscape Urban Plann.* 168, 94–116. doi: 10.1016/j.landurbplan.2017.09.019
- Liu, Y., Mei, X., Yue, L., and Zhang, M. (2025). Response of carbon storage to land use change and multi-scenario predictions in Zunyi, China. *Sci. Rep.* 15, 236. doi: 10.1038/s41598-024-81444-5
- Lyu, K., and Li, Z. (2025). Scenario based assessment of carbon storage and habitat quality under land use change in Shandong Province China. *Sci. Rep.* 15, 38098. doi: 10.1038/s41598-025-25097-y
- Mallapaty, S. (2020). How China could be carbon neutral by mid-century. *Nature* 586, 482–483. doi: 10.1038/d41586-020-02927-9
- Nie, X., Lu, B., Chen, Z., Yang, Y., Chen, S., Chen, Z., et al. (2020). Increase or decrease? Integrating the CLUMondo and InVEST models to assess the impact of the implementation of the Major Function Oriented Zone planning on carbon storage. *Ecol. Indic.* 118, 106708. doi: 10.1016/j.ecolind.2020.106708
- Sharp, R., Chaplin-Kramer, R., Wood, S., Guerry, A., Tails, H., and Ricketts, T. (2018). “In VEST User’s Guide,” in *Stanford, CA, USA: The Natural Capital Project*.
- Tang, Z., Ning, R., Wang, D., Tian, X., Bi, X., Zhou, Z., et al. (2024). Carbon stocks in coastal wetlands of the Yellow River Delta and their response to future multi-scenarios. *Acta Ecol. Sin.* 44, 3280–3292. doi: 10.20103/j.stxb.202308211801
- Wan, L., Liu, X., Guo, H., Xue, W., Liu, K., Lii, L., et al. (2025). Spatio-temporal succession and prediction of carbon storage in ecological conservation area of western Beijing based on InVEST-PLUS model. *Geological Bull. China* 44, 1272–1284. doi: 10.12097/gbc.2024.10.049
- Wang, B. (2023). Spatial-temporal pattern evolution and multi-scenario simulation of land use conflict in Poyang Lake Area based on PLUS model.
- Wang, Z., Zhong, A., Wei, E., and Hu, C. (2024). Carbon storage simulation and land use optimization for high-water-table resource-based cities based on the coupled GMOP-PLUS-InVEST model. *Remote Sens.* 16, 4480. doi: 10.3390/rs16234480
- Wei, M., Du, C., and Wang, X. (2023). Analysis and forecast of land use and carbon sink changes in Jilin Province, China. *Sustainability* 15, 14040. doi: 10.3390/su151914040
- Xu, L., He, N., and Yu, G. (2018). “A dataset of carbon density in Chinese terrestrial ecosystems, (2010s),” in *Beijing: Science Data Bank*. doi: 10.11922/csdata.2018.0026.zh
- Xu, X., Li, K., Li, C., Han, F., Zhao, J., and Li, Y. (2025). Spatial and chronological assessment of variations in carbon stocks in land-based ecosystems in Shandong Province and prospective predictions, (1990 to 2040). *Sustainability* 17, 2424. doi: 10.3390/su17062424
- Yang, J., and Huang, X. (2021). The 30 m annual land cover datasets and its dynamics in China from 1990 to 2020 (1.0.0). doi: 10.5194/essd-2021-7
- Yang, X., Qian, B., Ji, G., Chen, W., Huang, J., Guo, Y., et al. (2024). Characteristics of spatial and temporal changes in carbon stocks in the middle and upper reaches of the Huaihe River Basin and future multi-scenario simulation prediction. *Environ. Sci.* 45, 5970–5982. doi: 10.13227/j.hjck.202311034
- Zhang, X., Li, Z., Lin, J., Zhao, L., and Wang, Z. (2025). Simulation of multi-scenario land use change and carbon storage in the Yihe River Basin. *Environ. Sci.* 1–21. doi: 10.13227/j.hjck.202505355
- Zhang, Z., Zhu, Y., and Jia, P. (2024). Ecological protection redlines’ positive impact on terrestrial carbon storage in Hainan Island, China. *Land* 13, 1292. doi: 10.3390/land13081292
- Zheng, H., and Zheng, H. (2023). Assessment and prediction of carbon storage based on land use/land cover dynamics in the coastal area of Shandong Province. *Ecol. Indic.* 153, 110474. doi: 10.1016/j.ecolind.2023.110474
- Zhu, G., Qiu, D., Zhang, Z., Sang, L., Liu, Y., Wang, L., et al. (2021). Land-use changes lead to a decrease in carbon storage in arid region, China. *Ecol. Indic.* 127, 107770. doi: 10.1016/j.ecolind.2021.107770
- Zhu, L., Song, R., Sun, S., Li, Y., and Hu, K. (2022). Land use/land cover change and its impact on ecosystem carbon storage in coastal areas of China from 1980 to 2050. *Ecol. Indic.* 142, 109178. doi: 10.1016/j.ecolind.2022.109178
- Zhu, Z., Zhao, S., Li, Q., Shi, Z., Wu, Y., and Wang, L. (2025). Spatiotemporal evolution and prediction of land use change and carbon storage in ionic rare earth mining areas based on the YOLOv11–SegFormer–InVEST–PLUS integrated model. *Ecol. Indic.* 178, 113983. doi: 10.1016/j.ecolind.2025.113983